applied sciences

MDPI

Article

Optical Bullets and Their Modulational Instability Analysis

Khalil S. Al-Ghafri [1,*], Edamana V. Krishnan [2], Salam Khan [3] and Anjan Biswas [4,5,6,7,8]

[1] College of Applied Sciences, University of Technology and Applied Sciences, P.O. Box 14, Ibri 516, Oman
[2] Department of Mathematics, Sultan Qaboos University, P.O. Box 36, Al-Khod 123, Oman
[3] Department of Physics, Chemistry and Mathematics, Alabama A&M University, Normal, AL 35762, USA
[4] Department of Mathematics and Physics, Grambling State University, Grambling, LA 71245, USA
[5] Mathematical Modeling and Applied Computation (MMAC) Research Group, Department of Mathematics, King Abdulaziz University, Jeddah 21589, Saudi Arabia
[6] Department of Applied Mathematics, National Research Nuclear University, 31 Kashirskoe Hwy, 115409 Moscow, Russia
[7] Department of Applied Sciences, Cross-Border Faculty, Dunarea de Jos University of Galati, 111 Domneasca Street, 800201 Galati, Romania
[8] Department of Mathematics and Applied Mathematics, Sefako Makgatho Health Sciences University, Medunsa 0204, South Africa
* Correspondence: khalil.ibr@cas.edu.om

Abstract: The current work is devoted to investigating the multidimensional solitons known as optical bullets in optical fiber media. The governing model is a (3+1)-dimensional nonlinear Schrödinger system (3D-NLSS). The study is based on deriving the traveling wave reduction from the 3D-NLSS that constructs an elliptic-like equation. The exact solutions of the latter equation are extracted with the aid of two analytic approaches, the projective Riccati equations and the Bernoulli differential equation. Upon applying both methods, a plethora of assorted solutions for the 3D-NLSS are created, which describe mixed optical solitons having the profiles of bright, dark, and singular solitons. Additionally, the employed techniques provide several kinds of periodic wave solutions. The physical structures of some of the derived solutions are depicted to interpret the nature of the medium characterized by the 3D-NLSS. In addition, the modulation instability of the discussed model is examined by making use of the linear stability analysis.

Keywords: modulation instability; optical bullets; (3+1)-dimensional nonlinear Schrödinger system; projective Riccati equations method; Bernoulli sub-equation function method

Citation: Al-Ghafri, K.S.; Krishnan, E.V.; Khan, S.; Biswas, A. Optical Bullets and Their Modulational Instability Analysis. *Appl. Sci.* **2022**, *12*, 9221. https://doi.org/10.3390/app12189221

Received: 24 July 2022
Accepted: 13 September 2022
Published: 14 September 2022

1. Introduction

Wave phenomena have become one of the mechanisms that helps to understand the nature of the medium in which they arise [1–5]. The structures of waves varies enormously and takes different forms based on the physical properties of the media. In addition, the continuous theoretical and experimental studies of wave features have led to considerable development and steady progress toward physical and industrial applications in different branches of science such as fluid dynamics, plasma physics, nonlinear optics, quantum electronics, signal processing, and many others [6–10]. Recently, the soliton has been considered one of the ubiquitous waves that has made a contribution to enhancing modern technology and applied sciences [11–19]. Shedding light on the field of nonlinear optics, solitons, which are stable and undistorted pulses arising due to the balance between the dispersion and nonlinearity, have been found to play a vital role in developing an electronic communication system where this type of wave efficiently transmits information through optical fiber over long distances. To examine the dynamic of solitons, various models that belong to the class of nonlinear Schrödinger equation (NLSE) have been developed and studied widely during the past decade, taking into account the distinct physical effects in the medium. For instance, the NLSE with different forms of nonlinear influences or in the

presence of higher-order dispersion has been investigated by many experts and scholars to observe soliton behaviors in optical fibers [20–23]. The detection of ultrashort pulses, as an example of soliton propagation in optical fiber, that have a significant impact on developing photonic and optoelectronic devices can be carried out through studying the generalized NLSE of third order [24,25]. There have been many studies conducted on the features and structures of optical solitons in fiber medium; see e.g., [26–30]. In multidimensional optical media, solitons are also known as optical bullets; this term was firstly introduced by Silberberg in 1989 [31]. Mostly, the dominant model for generating optical bullets is the 3-dimensional NLSE. In contrast to self-focusing effects that tend to squeeze the pulse, both diffraction and dispersion cause spreading of the pulse. Subsequently, the balance between these two contradictory processes leads to the formation of this type of optical soliton. Optical bullets have different behaviors from solitons, where the former experience the loss of energy during collision events, and the latter survive collisions without losing energy [32]. In the literature, Soto-Crespo et al. [33] detected optical light bullets in nonlinear dissipative media that were governed by the (3+1)-dimensional complex cubic–quintic Ginzburg–Landau equation. They demonstrated that stable bullets had bell-shaped solitons, whereas unstable bullets were transformed into the shape of rockets. Furthermore, the formation of light bullets upon ultrashort laser pulse filamentation in dissipative media such as air, fused silica, fluorite, etc., has been studied in the presence of different physical effects, see [34–38]. For more examples of investigating the propagation characteristics of optical bullets, the reader is referred to the following studies [39–47].

Recently, several researchers have explored miscellaneous types of wave forms for an integrable system of coupled (2+1)-dimensional NLSE (2D-NLSS) given as

$$\begin{aligned} &i\mathrm{Y}_t = \mathrm{Y}_{xy} + \mathrm{Y}\Gamma, \\ &\Gamma_x = 2(|\mathrm{Y}|^2)_y, \end{aligned} \tag{1}$$

where Y and Γ represent complex and real functions, respectively, and both of them are functions of the variables x, y, and t. On one side, Model (1) reduces to the NLSE as $\partial_x = \partial_y$, and on the other side, it is converted into the complex sine–Gordon equation when $\partial_t = 0$. The bilinear form of 2D-NLSS was derived by Radha and Lakshmanan [48] so as to obtain soliton solutions. Further to this, numerous authors have extracted breather and rogue wave solutions [49–52]. Additionally, optical wave solutions of different forms including bright soliton, dark soliton, periodic waves, and others have been found as well [53–57].

The model of the nonlinear Schrödinger system in (3+1) dimensions (3D-NLSS) has also been discussed by a few authors, and it is addressed as

$$\begin{aligned} &i\mathrm{Y}_t = \mathrm{Y}_{xy} + \mathrm{Y}_{xz} + \mathrm{Y}\Gamma, \\ &\Gamma_x = 2\Big[(|\mathrm{Y}|^2)_y + (|\mathrm{Y}|^2)_z\Big]. \end{aligned} \tag{2}$$

Using the bilinear Hirota form, Borzykh [58] constructed a 1-soliton solution to the 3D-NLSS. Moreover, Zhang and Shen [59] studied Equation (2) by applying Bäcklund transformations and the variable separation approach. They arrived at new exact solutions to the 3D-NLSS. It has to be noted that the cubic nonlinear Schrödinger equation is valid for moderate nonlinearities, while the higher order of nonlinearities demands a higher order of the NLSE.

The main purpose of our study is to investigate various optical bullet solutions, which have not been examined previously for the 3D-NLSS (2). Different to the previous studies, the model of the 3D-NLSS is analyzed here using the traveling wave theory. The resulting elliptic-like equation is scrutinized by utilizing two integration schemes known as the projective Riccati equations method (PREM) and the Bernoulli sub-equation function method (BSEFM). The remaining sections of this paper detail the work as follows. Section 2 describes the steps to carry out the approaches to the solution. The variable transformation of a traveling wave form is employed in Section 3 to analyze the 3D-NLSS, and we elu-

cidate in Section 4 the derivation of the exact solutions to the 3D-NLSS via the proposed techniques. Section 5 studies the modulation instability of the 3D-NLSS by applying the linear stability analysis. In Section 6, the obtained results are discussed through showing graphical representations of some of the extracted solutions. The final section contains our conclusions.

2. Overview of Schemes

Our aim in this section is to clearly explain the strategy of using the solution methods, which are PREM and BSEFM, to solve the mathematical models. Assuming that a nonlinear evolution equation (NLEE) has the form [60,61]

$$G(q, q_t, q_x, q_{xx}, q_{xt}, q_{tt}, q_{xxx} \dots) = 0. \tag{3}$$

Here, $q = q(x,t)$ is an unknown function while G is a polynomial in q and its various partial derivatives.

Since this study intends to derive traveling wave solutions, the variable transformation is employed and identified by

$$q(x,t) = w(\xi), \qquad \xi = x - ct. \tag{4}$$

The transformation (4) changes the NLEE (3) into a nonlinear ordinary differential equation (NLODE) presented by

$$Q(w, w', w'', w''', \dots) = 0, \tag{5}$$

where the symbol $'$ means the derivative with respect to ξ.

2.1. Description of PREM

Consider that the solution of Equation (5) possesses the form

$$w(\xi) = a_0 + \sum_{i=1}^{m} f^{i-1}(\xi)[a_i f(\xi) + b_i g(\xi)], \tag{6}$$

where $f = f(\xi)$ and $g = g(\xi)$ satisfy the projective Riccati equations given by

$$\begin{aligned} f'(\xi) = pf(\xi)g(\xi), \qquad g'(\xi) = R + pg^2(\xi) - rf(\xi), \\ g^2(\xi) = -p\left[R - 2rf(\xi) + \frac{r^2+\delta}{R} f^2(\xi)\right], \end{aligned} \tag{7}$$

where R and r are real constants, and $p = \delta = \pm 1$. The set of Equation (7) is found to accept the following solutions.

Case 1. If $p = -1, R \neq 0$,

$$f_1(\xi) = \frac{RA}{B\cosh(\xi) + C\sinh(\xi) + Ar}, \quad g_1(\xi) = \frac{\sqrt{R}\{B\sinh(\sqrt{R}\xi) + C\cosh(\sqrt{R}\xi)\}}{B\cosh(\sqrt{R}\xi) + C\sinh(\sqrt{R}\xi) + Ar}, \tag{8}$$

where $A, B,$ and$C$ satisfy $C^2 = A^2 + B^2$ as $\delta = 1$, and $A, B,$ and$C$ satisfy $B^2 = A^2 + C^2$ as $\delta = -1$.

$$f_2(\xi) = \frac{R}{\sinh(\sqrt{R}\xi) + r}, \qquad g_2(\xi) = \frac{\sqrt{R}\cosh(\sqrt{R}\xi)}{\sinh(\sqrt{R}\xi) + r}, \tag{9}$$

demands $\delta = 1$.

$$f_3(\xi) = \frac{R}{\cosh(\sqrt{R}\xi) + r}, \qquad g_3(\xi) = \frac{\sqrt{R}\sinh(\sqrt{R}\xi)}{\cosh(\sqrt{R}\xi) + r}, \tag{10}$$

implies $\delta = -1$.

Case 2. If $p = 1, R \neq 0$,

$$f_4(\xi) = \frac{RA}{B\cos(\sqrt{R}\xi) + C\sin(\sqrt{R}\xi) + Ar}, \quad g_4(\xi) = \frac{\sqrt{R}\{B\sin(\sqrt{R}\xi) - C\cos(\sqrt{R}\xi)\}}{B\cos(\sqrt{R}\xi) + C\sin(\sqrt{R}\xi) + Ar}, \tag{11}$$

where A, B, and C satisfy $A^2 = -B^2 - C^2$ as $\delta = 1$, and A, B, and C satisfy $A^2 = B^2 + C^2$ as $\delta = -1$.

$$f_5(\xi) = \frac{R}{\sin(\sqrt{R}\xi) + r}, \qquad g_5(\xi) = -\frac{\sqrt{R}\cos(\sqrt{R}\xi)}{\sin(\sqrt{R}\xi) + r}, \tag{12}$$

$$f_6(\xi) = \frac{R}{\cos(\sqrt{R}\xi) + r}, \qquad g_6(\xi) = \frac{\sqrt{R}\sin(\sqrt{R}\xi)}{\cos(\sqrt{R}\xi) + r}, \tag{13}$$

where (12) and (13) demand $\delta = -1$.

Case 3. If $R = r = 0$,

$$f_7(\xi) = \frac{s_1}{-p\xi + s_2} = s_1 g_7(\xi), \qquad g_7(\xi) = \frac{1}{-p\xi + s_2}, \tag{14}$$

where s_1 and s_2 are arbitrary constants.

Substituting (6) along with (7) into Equation (5), a polynomial in the variables $f^j(\xi)$ and $f^{j-1}(\xi)\,g(\xi)$ is obtained. Then, equating each coefficient of $f^j(\xi)$ and $f^{j-1}(\xi)\,g(\xi)$ in this polynomial to zero generates a system of algebraic equations for a_j, b_j. Finally, the solutions to this system of equations create various exact solutions to Equation (3) with reference to (8)–(14).

2.2. Elucidation of BSEFM

Let Equation (5) have a solution expressed in the form

$$w(\xi) = \sum_{j=1}^{n} l_j H^j = l_0 + l_1 H + l_2 H^2 + \cdots + l_n H^n, \tag{15}$$

where $H = H(\xi)$ satisfies the Bernoulli differential equation given by

$$H' = bH + dH^k, \tag{16}$$

where $b \neq 0, d \neq 0, k \in \mathbb{R} - 0, 1, 2$. Equation (16) admits the following solutions presented as

$$H(\xi) = \left[\frac{-d}{b} + \frac{h}{e^{b(k-1)\xi}}\right]^{\frac{1}{1-k}}, b \neq d, \tag{17}$$

$$H(\xi) = \left[\frac{(h-1) + (h+1)\tanh\left(\frac{b(1-k)\xi}{2}\right)}{1 - \tanh\left(\frac{b(1-k)\xi}{2}\right)}\right]^{\frac{1}{1-k}}, b = d,\ h \in \mathbb{R}. \tag{18}$$

Inserting (15) into Equation (5) and using (16), one can find a polynomial in H. Equating all the coefficients of same power of H to zero brings about a system of equations. Solving this system algebraically provides the values of l_j $(j = 0, \ldots, n)$. At the end of this strategy, we arrive at new forms of solutions to Equation (3).

3. Mathematical Analysis of the Model

The investigation of the optical bullet solutions to the 3D-NLSS (2) demands reducing it to NLODE in order to apply the proposed solution techniques. To start, we consider the transformation of the traveling wave form given by

$$\begin{aligned} \Upsilon(x,y,z,t) &= u(\xi)e^{i\Phi(x,y,z,t)}, \\ \Gamma(x,y,z,t) &= v(\xi). \end{aligned} \tag{19}$$

Here, the variable ξ is the traveling coordinate defined as

$$\xi = \alpha x + \beta y + \gamma z + \nu t, \tag{20}$$

and the function $\Phi(x,y,z,t)$ stands for the phase component introduced as

$$\Phi(x,y,t) = \lambda x + \eta y + \sigma z + \omega t, \tag{21}$$

where $\alpha, \beta, \gamma, \nu, \lambda, \eta, \sigma$, and ω are arbitrary constants.

Making use of the transformation (19), Equation (2) reduces to

$$i(\nu - \alpha\eta - \beta\lambda - \alpha\sigma - \lambda\gamma)u' - \alpha(\beta+\gamma)u'' - (\omega - \lambda\eta - \lambda\sigma)u - uv = 0, \tag{22}$$

$$\alpha v' = 4(\beta+\gamma)uu', \tag{23}$$

where $u = u(\xi)$, and $v = v(\xi)$. We deduce from integrating Equation (23) an equation of the form

$$v = 2\frac{(\beta+\gamma)}{\alpha}u^2, \tag{24}$$

where the constant of integration is considered to be zero. The substitution of Equation (24) into Equation (22) yields

$$i(\nu - \alpha\eta - \beta\lambda - \alpha\sigma - \lambda\gamma)u' - \alpha(\beta+\gamma)u'' - (\omega - \lambda\eta - \lambda\sigma)u - 2\frac{(\beta+\gamma)}{\alpha}u^3 = 0. \tag{25}$$

Separating the last equation into the real and imaginary parts results in

$$\alpha(\beta+\gamma)u'' + (\omega - \lambda\eta - \lambda\sigma)u + 2\frac{(\beta+\gamma)}{\alpha}u^3 = 0, \tag{26}$$

$$(\nu - \alpha\eta - \beta\lambda - \alpha\sigma - \lambda\gamma)u' = 0. \tag{27}$$

One can readily induce from Equation (27) the constraint condition given by

$$\nu = \alpha\eta + \beta\lambda + \alpha\sigma + \lambda\gamma. \tag{28}$$

Hence, the optical soliton solutions of the 3D-NLSS are retrieved by dealing with the elliptic-like equation presented as

$$A_0u'' + A_1u + A_3u^3 = 0, \tag{29}$$

where the constants A_0, A_1, and A_3 are defined by

$$A_0 = \alpha(\beta+\gamma), \tag{30}$$

$$A_1 = \omega - \lambda\eta - \lambda\sigma, \tag{31}$$

$$A_3 = 2\frac{(\beta+\gamma)}{\alpha}. \tag{32}$$

4. Optical Bullet Solutions

This section concentrates on constructing various structures of optical bullet solutions for the system of Equation (2) utilizing the two proposed mathematical approaches, namely, PREM and BSEFM for solving Equation (29).

4.1. Solving by PREM

The series form based on the solutions of projective Riccati equations is exploited here to derive the solutions of Equation (29), which are mutated by (19) to optical wave solutions for the model (2). Balancing between the terms u'' and u^3 in Equation (29) leads to $m = 1$. According to (6), the general solution form of Equation (29) reads

$$u(\xi) = a_0 + a_1 f + b_1 g. \tag{33}$$

Substituting (33) along with (7) into (29), combining all the terms having the same exponent of $f^i g^j$ together, and equating each coefficient to zero leads to a system of algebraic equations. Solving the resulting system gives rise to three sets of solutions that reveal distinct cases of solutions for the model (2).

Set I.

$$a_0 = 0, \quad a_1 = \frac{A_0}{2}\sqrt{-\frac{r^2+\delta}{A_1 A_3}}, \quad b_1 = \sqrt{-\frac{A_0}{2A_3}}, \quad R = -\frac{2pA_1}{A_0}, \quad p = \pm 1, \quad \delta = \pm 1. \tag{34}$$

Case I1. If $p = -1$, from (34) along with (8)–(10), one can find optical soliton solutions for Equation (2) as

$$\begin{aligned}
\Upsilon(x,y,z,t) &= \pm\sqrt{-\frac{A_1}{A_3}}\left[\frac{A\sqrt{r^2+\delta} + B\sinh(\sqrt{\frac{2A_1}{A_0}}\xi) + C\cosh(\sqrt{\frac{2A_1}{A_0}}\xi)}{B\cosh(\sqrt{\frac{2A_1}{A_0}}\xi) + C\sinh(\sqrt{\frac{2A_1}{A_0}}\xi) + Ar}\right] e^{i\Phi(x,y,z,t)}, \\
\Gamma(x,y,z,t) &= -A_1\left[\frac{A\sqrt{r^2+\delta} + B\sinh(\sqrt{\frac{2A_1}{A_0}}\xi) + C\cosh(\sqrt{\frac{2A_1}{A_0}}\xi)}{B\cosh(\sqrt{\frac{2A_1}{A_0}}\xi) + C\sinh(\sqrt{\frac{2A_1}{A_0}}\xi) + Ar}\right]^2,
\end{aligned} \tag{35}$$

where $C^2 = A^2 + B^2$ when $\delta = 1$, and $B^2 = A^2 + C^2$ when $\delta = -1$.

$$\begin{aligned}
\Upsilon(x,y,z,t) &= \pm\sqrt{-\frac{A_1}{A_3}}\left[\frac{\sqrt{r^2+1} + \cosh(\sqrt{\frac{2A_1}{A_0}}\xi)}{\sinh(\sqrt{\frac{2A_1}{A_0}}\xi) + r}\right] e^{i\Phi(x,y,z,t)}, \\
\Gamma(x,y,z,t) &= -A_1\left[\frac{\sqrt{r^2+1} + \cosh(\sqrt{\frac{2A_1}{A_0}}\xi)}{\sinh(\sqrt{\frac{2A_1}{A_0}}\xi) + r}\right]^2,
\end{aligned} \tag{36}$$

where solution (36) demands $\delta = 1$.

$$\begin{aligned}
\Upsilon(x,y,z,t) &= \pm\sqrt{-\frac{A_1}{A_3}}\left[\frac{\sqrt{r^2-1} + \sinh(\sqrt{\frac{2A_1}{A_0}}\xi)}{\cosh(\sqrt{\frac{2A_1}{A_0}}\xi) + r}\right] e^{i\Phi(x,y,z,t)}, \\
\Gamma(x,y,z,t) &= -A_1\left[\frac{\sqrt{r^2-1} + \sinh(\sqrt{\frac{2A_1}{A_0}}\xi)}{\cosh(\sqrt{\frac{2A_1}{A_0}}\xi) + r}\right]^2,
\end{aligned} \tag{37}$$

where solution (37) is obtained when $\delta = -1$.

Case I2. If $p = 1$, from (34) in company with (8)–(10), we arrive at periodic wave solutions for Equation (2) presented by

$$\Upsilon(x,y,z,t) = \pm\sqrt{\frac{A_1}{A_3}}\left[\frac{A\sqrt{-(r^2+\delta)} + B\sin(\sqrt{-\frac{2A_1}{A_0}}\xi) - C\cos(\sqrt{-\frac{2A_1}{A_0}}\xi)}{B\cos(\sqrt{-\frac{2A_1}{A_0}}\xi) + C\sin(\sqrt{-\frac{2A_1}{A_0}}\xi) + Ar}\right]e^{i\Phi(x,y,z,t)},$$
$$\Gamma(x,y,z,t) = A_1\left[\frac{A\sqrt{-(r^2+\delta)} + B\sin(\sqrt{-\frac{2A_1}{A_0}}\xi) - C\cos(\sqrt{-\frac{2A_1}{A_0}}\xi)}{B\cos(\sqrt{-\frac{2A_1}{A_0}}\xi) + C\sin(\sqrt{-\frac{2A_1}{A_0}}\xi) + Ar}\right]^2, \tag{38}$$

where $A^2 = -(B^2 + C^2)$ when $\delta = 1$, and $A^2 = B^2 + C^2$ when $\delta = -1$.

$$\Upsilon(x,y,z,t) = \pm\sqrt{\frac{A_1}{A_3}}\left[\frac{\sqrt{-(r^2-1)} + \cos(\sqrt{-\frac{2A_1}{A_0}}\xi)}{\sin(\sqrt{-\frac{2A_1}{A_0}}\xi) + r}\right]e^{i\Phi(x,y,z,t)},$$
$$\Gamma(x,y,z,t) = A_1\left[\frac{\sqrt{-(r^2-1)} + \cos(\sqrt{-\frac{2A_1}{A_0}}\xi)}{\sin(\sqrt{-\frac{2A_1}{A_0}}\xi) + r}\right]^2, \tag{39}$$

$$\Upsilon(x,y,z,t) = \pm\sqrt{\frac{A_1}{A_3}}\left[\frac{\sqrt{-(r^2-1)} + \sin(\sqrt{-\frac{2A_1}{A_0}}\xi)}{\cos(\sqrt{-\frac{2A_1}{A_0}}\xi) + r}\right]e^{i\Phi(x,y,z,t)},$$
$$\Gamma(x,y,z,t) = A_1\left[\frac{\sqrt{-(r^2-1)} + \sin(\sqrt{-\frac{2A_1}{A_0}}\xi)}{\cos(\sqrt{-\frac{2A_1}{A_0}}\xi) + r}\right]^2, \tag{40}$$

where solutions (39) and (40) demand $\delta = -1$.

Set II.

$$a_0 = b_1 = 0, \quad a_1 = A_0\sqrt{\frac{2\delta}{A_1A_3}}, \quad R = \frac{pA_1}{A_0}, \quad r = 0, \quad p = \pm1, \quad \delta = \pm1. \tag{41}$$

Case II1. If $p = -1$, from (41) along with (8)–(10), this leads to optical soliton solutions for Equation (2) given by

$$\Upsilon(x,y,z,t) = \pm\sqrt{\frac{2\delta A_1}{A_3}}\left[\frac{A}{B\cosh(\sqrt{-\frac{A_1}{A_0}}\xi) + C\sinh(\sqrt{-\frac{A_1}{A_0}}\xi)}\right]e^{i\Phi(x,y,z,t)},$$
$$\Gamma(x,y,z,t) = 2\delta A_1\left[\frac{A}{B\cosh(\sqrt{-\frac{A_1}{A_0}}\xi) + C\sinh(\sqrt{-\frac{A_1}{A_0}}\xi)}\right]^2, \tag{42}$$

where $C^2 = A^2 + B^2$ when $\delta = 1$, and $B^2 = A^2 + C^2$ when $\delta = -1$.

$$\Upsilon(x,y,z,t) = \pm\sqrt{\frac{2A_1}{A_3}}\left[\frac{1}{\sinh(\sqrt{-\frac{A_1}{A_0}}\xi)}\right]e^{i\Phi(x,y,z,t)},$$
$$\Gamma(x,y,z,t) = 2A_1\left[\frac{1}{\sinh(\sqrt{-\frac{A_1}{A_0}}\xi)}\right]^2, \tag{43}$$

where solution (43) demands $\delta = 1$.

$$\begin{aligned} \Upsilon(x,y,z,t) &= \pm\sqrt{-\frac{2A_1}{A_3}}\left[\frac{1}{\cosh(\sqrt{-\frac{A_1}{A_0}}\xi)}\right]e^{i\Phi(x,y,z,t)}, \\ \Gamma(x,y,z,t) &= -2A_1\left[\frac{1}{\cosh(\sqrt{-\frac{A_1}{A_0}}\xi)}\right]^2, \end{aligned} \tag{44}$$

where solution (44) implies $\delta = -1$.

Case II2. If $p = 1$, from (41) together with (8)–(10), we procure periodic wave solutions for Equation (2) as

$$\begin{aligned} \Upsilon(x,y,z,t) &= \pm\sqrt{\frac{2\delta A_1}{A_3}}\left[\frac{A}{B\cos(\sqrt{\frac{A_1}{A_0}}\xi) + C\sin(\sqrt{\frac{A_1}{A_0}}\xi)}\right]e^{i\Phi(x,y,z,t)}, \\ \Gamma(x,y,z,t) &= 2\delta A_1\left[\frac{A}{B\cos(\sqrt{\frac{A_1}{A_0}}\xi) + C\sin(\sqrt{\frac{A_1}{A_0}}\xi)}\right]^2, \end{aligned} \tag{45}$$

where $A^2 = -(B^2 + C^2)$ when $\delta = 1$, and $A^2 = B^2 + C^2$ when $\delta = -1$.

$$\begin{aligned} \Upsilon(x,y,z,t) &= \pm\sqrt{-\frac{2A_1}{A_3}}\left[\frac{1}{\sin(\sqrt{\frac{A_1}{A_0}}\xi)}\right]e^{i\Phi(x,y,z,t)}, \\ \Gamma(x,y,z,t) &= -2A_1\left[\frac{1}{\sin(\sqrt{\frac{A_1}{A_0}}\xi)}\right]^2, \end{aligned} \tag{46}$$

$$\begin{aligned} \Upsilon(x,y,z,t) &\pm \sqrt{-\frac{2A_1}{A_3}}\left[\frac{1}{\cos(\sqrt{\frac{A_1}{A_0}}\xi)}\right]e^{i\Phi(x,y,z,t)}, \\ \Gamma(x,y,z,t) &= -2A_1\left[\frac{1}{\cos(\sqrt{\frac{A_1}{A_0}}\xi)}\right]^2, \end{aligned} \tag{47}$$

where solutions (46) and (47) need $\delta = -1$.

Set III.

$$a_0 = a_1 = 0, \quad b_1 = \sqrt{-\frac{2A_0}{A_3}}, \quad R = -\frac{pA_1}{2A_0}, \quad r = 0, \quad p = \pm 1, \quad \delta = \pm 1. \tag{48}$$

Case III1. If $p = -1$, from (48) along with (8)–(10), this provides optical soliton solutions for Equation (2) given by

$$\begin{aligned} \Upsilon(x,y,z,t) &= \pm\sqrt{-\frac{A_1}{A_3}}\left[\frac{B\sinh(\sqrt{\frac{A_1}{2A_0}}\xi) + C\cosh(\sqrt{\frac{A_1}{2A_0}}\xi)}{B\cosh(\sqrt{\frac{A_1}{2A_0}}\xi) + C\sinh(\sqrt{\frac{A_1}{2A_0}}\xi)}\right]e^{i\Phi(x,y,z,t)}, \\ \Gamma(x,y,z,t) &= -A_1\left[\frac{B\sinh(\sqrt{\frac{A_1}{2A_0}}\xi) + C\cosh(\sqrt{\frac{A_1}{2A_0}}\xi)}{B\cosh(\sqrt{\frac{A_1}{2A_0}}\xi) + C\sinh(\sqrt{\frac{A_1}{2A_0}}\xi)}\right]^2, \end{aligned} \tag{49}$$

$$\begin{aligned}
\Upsilon(x,y,z,t) &= \pm\sqrt{-\frac{A_1}{A_3}}\left[\frac{\cosh(\sqrt{\frac{A_1}{2A_0}}\xi)}{\sinh(\sqrt{\frac{A_1}{2A_0}}\xi)}\right]e^{i\Phi(x,y,z,t)},\\
\Gamma(x,y,z,t) &= -A_1\left[\frac{\cosh(\sqrt{\frac{A_1}{2A_0}}\xi)}{\sinh(\sqrt{\frac{A_1}{2A_0}}\xi)}\right]^2,
\end{aligned} \tag{50}$$

$$\begin{aligned}
\Upsilon(x,y,z,t) &= \pm\sqrt{-\frac{A_1}{A_3}}\left[\frac{\sinh(\sqrt{\frac{A_1}{2A_0}}\xi)}{\cosh(\sqrt{\frac{A_1}{2A_0}}\xi)}\right]e^{i\Phi(x,y,z,t)},\\
\Gamma(x,y,z,t) &= -A_1\left[\frac{\sinh(\sqrt{\frac{A_1}{2A_0}}\xi)}{\cosh(\sqrt{\frac{A_1}{2A_0}}\xi)}\right]^2.
\end{aligned} \tag{51}$$

Case III2. If $p = 1$, from (48) in company with (8)–(10), we derive periodic wave solutions for Equation (2) as

$$\begin{aligned}
\Upsilon(x,y,z,t) &= \pm\sqrt{\frac{A_1}{A_3}}\left[\frac{B\sin(\sqrt{-\frac{A_1}{2A_0}}\xi)-C\cos(\sqrt{-\frac{A_1}{2A_0}}\xi)}{B\cos(\sqrt{-\frac{A_1}{2A_0}}\xi)+C\sin(\sqrt{-\frac{A_1}{2A_0}}\xi)}\right]e^{i\Phi(x,y,z,t)},\\
\Gamma(x,y,z,t) &= A_1\left[\frac{B\sin(\sqrt{-\frac{A_1}{2A_0}}\xi)-C\cos(\sqrt{-\frac{A_1}{2A_0}}\xi)}{B\cos(\sqrt{-\frac{A_1}{2A_0}}\xi)+C\sin(\sqrt{-\frac{A_1}{2A_0}}\xi)}\right]^2,
\end{aligned} \tag{52}$$

$$\begin{aligned}
\Upsilon(x,y,z,t) &= \pm\sqrt{\frac{A_1}{A_3}}\left[\frac{\cos(\sqrt{-\frac{A_1}{2A_0}}\xi)}{\sin(\sqrt{-\frac{A_1}{2A_0}}\xi)}\right]e^{i\Phi(x,y,z,t)},\\
\Gamma(x,y,z,t) &= A_1\left[\frac{\cos(\sqrt{-\frac{A_1}{2A_0}}\xi)}{\sin(\sqrt{-\frac{A_1}{2A_0}}\xi)}\right]^2,
\end{aligned} \tag{53}$$

$$\begin{aligned}
\Upsilon(x,y,z,t) &= \pm\sqrt{\frac{A_1}{A_3}}\left[\frac{\sin(\sqrt{-\frac{A_1}{2A_0}}\xi)}{\cos(\sqrt{-\frac{A_1}{2A_0}}\xi)}\right]e^{i\Phi(x,y,z,t)},\\
\Gamma(x,y,z,t) &= A_1\left[\frac{\sin(\sqrt{-\frac{A_1}{2A_0}}\xi)}{\cos(\sqrt{-\frac{A_1}{2A_0}}\xi)}\right]^2.
\end{aligned} \tag{54}$$

Set IV.

$$a_0 = a_1 = 0, \quad b_1 = i\alpha, \quad r = R = 0, \quad p = \pm 1. \tag{55}$$

From (55) together with (8)–(10), we retrieve rational function solutions for Equation (2) in the form

$$\begin{aligned}
\Upsilon(x,y,z,t) &= \frac{i\alpha}{-p\xi+s_2}e^{i\Phi(x,y,z,t)},\\
\Gamma(x,y,z,t) &= \frac{-2\alpha(\beta+\gamma)}{(-p\xi+s_2)^2}.
\end{aligned} \tag{56}$$

4.2. Solving by BSEFM

Herein, the purpose is to extract the solution of the system (2) by implementing the Bernoulli sub-equation function method to Equation (29) as described in Section 2.2.

The balance between the terms u'' and u^3 in Equation (29) results in a relation between n and k given as

$$n = k - 1. \tag{57}$$

Taking $k = 3$ in Equation (57), this yields $n = 2$, and as a result the general form of the solution is given by

$$u(\xi) = l_0 + l_1 H + l_2 H^2. \tag{58}$$

Plugging (58) together with (16) into Equation (29), a polynomial of degree six in H is obtained. Gathering like terms with the same degree of H and setting each coefficient to zero, a system of algebraic equations is created. The solutions of this system give rise to the following cases of solutions for the 3D-NLSS (2).

Case 1. For $b \neq d$, it is found that

$$l_0 = \sqrt{-\frac{A_1}{A_3}}, \quad l_1 = 0, \quad l_2 = 2d\sqrt{-\frac{2A_0}{A_3}}, \quad b = \sqrt{-\frac{A_1}{2A_0}}. \tag{59}$$

These findings generate an optical soliton solution for Equation (2) as

$$\begin{aligned} \Upsilon(x,y,z,t) &= \pm\sqrt{-\frac{A_1}{A_3}}\,\frac{h\sqrt{\frac{A_1}{A_0}} + d\sqrt{2}\,e^{\sqrt{\frac{2A_1}{A_0}}\xi}}{h\sqrt{\frac{A_1}{A_0}} - d\sqrt{2}\,e^{\sqrt{\frac{2A_1}{A_0}}\xi}} e^{i\Phi(x,y,z,t)}, \\ \Gamma(x,y,z,t) &= -A_1\left[\frac{h\sqrt{\frac{A_1}{A_0}} + d\sqrt{2}\,e^{\sqrt{\frac{2A_1}{A_0}}\xi}}{h\sqrt{\frac{A_1}{A_0}} - d\sqrt{2}\,e^{\sqrt{\frac{2A_1}{A_0}}\xi}}\right]^2. \end{aligned} \tag{60}$$

Case 2. For $b = d$, we reach

$$l_0 = \sqrt{-\frac{A_1}{A_3}}, \quad l_1 = 0, \quad l_2 = 2\sqrt{-\frac{A_1}{A_3}}, \quad d = \sqrt{\frac{A_1}{2A_0}}. \tag{61}$$

From this consequence, we retrieve an optical soliton solution for Equation (2) as

$$\begin{aligned} \Upsilon(x,y,z,t) &= \pm\sqrt{-\frac{A_1}{A_3}}\,\frac{(h+1) - (h-1)\tanh\left(\sqrt{\frac{A_1}{2A_0}}\xi\right)}{(h-1) - (h+1)\tanh\left(\sqrt{\frac{A_1}{2A_0}}\xi\right)} e^{i\Phi(x,y,z,t)}, \\ \Gamma(x,y,z,t) &= -A_1\left[\frac{(h+1) - (h-1)\tanh\left(\sqrt{\frac{A_1}{2A_0}}\xi\right)}{(h-1) - (h+1)\tanh\left(\sqrt{\frac{A_1}{2A_0}}\xi\right)}\right]^2. \end{aligned} \tag{62}$$

5. Stability Analysis

The emergence of instability in a nonlinear wave medium that is known to occur because of the interaction between the dispersion and nonlinear influences results in the modulation of the steady-state. Thus, the technique of linear stability analysis can be exploited to study the modulation instability (MI) of the stationary solutions of 3D-NLSS (2). Therefore, we assume that the stationary solutions are defined as

$$\begin{aligned} \Upsilon(x,y,z,t) &= \rho e^{i\vartheta t}, \\ \Gamma(x,y,z,t) &= \mu, \end{aligned} \tag{63}$$

where ρ and μ are real constants. Inserting (63) into 3D-NLSS (2), one can deduce $\vartheta = -\mu$. To apply the standard linear stability analysis, perturbed fields are introduced in the amplitudes of stationary waves to find an expression given as

$$\begin{aligned} \Upsilon(x,y,z,t) &= (\rho + V)e^{-i\mu t}, \\ \Gamma(x,y,z,t) &= (\mu + W), \end{aligned} \tag{64}$$

where $V = V(x,y,z,t)$ and $W = W(x,y,z,t)$ are complex and real functions, respectively. Substituting (64) into 3D-NLSS (2), one can acquire the linearized disturbance equations of the form

$$\begin{aligned} iV_t &= V_{xy} + V_{xz} + \rho W, \\ W_x &= 2\rho[(V_y + V_y^*) + (V_z + V_z^*)], \end{aligned} \tag{65}$$

where * indicates the complex conjugate. Consider that the solutions of Equation (65) are written as

$$\begin{aligned} V &= \alpha_1 e^{i(\kappa_1 x + \kappa_2 y + \kappa_3 z - \varpi t)} + i\alpha_2 e^{-i(\kappa_1 x + \kappa_2 y + \kappa_3 z - \varpi t)}, \\ W &= (\beta_1 + i\beta_2)e^{i(\kappa_1 x + \kappa_2 y + \kappa_3 z - \varpi t)} + (\beta_1 - i\beta_2)e^{-i(\kappa_1 x + \kappa_2 y + \kappa_3 z - \varpi t)}, \end{aligned} \tag{66}$$

where κ_j $(j = 1,2,3)$ and ϖ are the normalized wave numbers and frequency of perturbation, respectively, while α_l and β_l $(l = 1,2)$ are the coefficients of linear combination. Upon applying the ansatz (66) to Equation (65), we reach the following four homogeneous equations as

$$\begin{aligned} &-(\kappa_1(\kappa_2 + \kappa_3) + \varpi)\alpha_1 + \rho\beta_1 + i\rho\beta_2 = 0, \\ &-i(\kappa_1(\kappa_2 + \kappa_3) - \varpi)\alpha_2 + \rho\beta_1 - i\rho\beta_2 = 0, \\ &-2i\rho(\kappa_2 + \kappa_3)\alpha_1 - 2\rho(\kappa_2 + \kappa_3)\alpha_2 + i\kappa_1\beta_1 - \kappa_1\beta_2 = 0, \\ &2i\rho(\kappa_2 + \kappa_3)\alpha_1 - 2\rho(\kappa_2 + \kappa_3)\alpha_2 - i\kappa_1\beta_1 - \kappa_1\beta_2 = 0. \end{aligned} \tag{67}$$

From the above system, we can construct a matrix for the coefficients of α_l and β_l $(l = 1,2)$. In order to assure nontrivial solutions for the system (67), the determinant of the matrix must be zero. Accordingly, the dispersion relation is produced as

$$\kappa_1^4(\kappa_2 + \kappa_3)^2 - \kappa_1^2\left(\varpi^2 + 4\rho^2(\kappa_2 + \kappa_3)^2\right) + 8\rho^4(\kappa_2 + \kappa_3)^2 = 0, \tag{68}$$

which has the solutions for ϖ in the form

$$\varpi = \pm\frac{(\kappa_2 + \kappa_3)}{\kappa_1}\sqrt{\left(\kappa_1^2 - 2\rho^2\right)^2 + 4\rho^4}. \tag{69}$$

Based on this expression, we can determine the situation of the MI for the 3D-NLSS (2). It is clearly seen that $(\kappa_1^2 - 2\rho^2)^2 + 4\rho^4$ is always ≥ 0, meaning that the MI does not exist because Im $\varpi = 0$. Eventually, the steady state is stable against wave number perturbations.

6. Results and Discussion

According to the obtained solutions of the 3D-NLSS in Section 4, it is worth mentioning that the proposed mathematical tools have been powerful in generating a plethora of exact solutions containing hyperbolic function, trigonometric function, and rational function solutions, which describe various wave types. An optical soliton is one of the extracted wave structures, and it includes the shapes of bright, dark, and singular solitons. Further to these wave forms, periodic waves that have dissimilar profiles are also retrieved.

To report the behavior of optical bullets and other waves, the graphical representations of some obtained solutions are given. Appropriate values for the model parameters are selected to draw the 3D plot for the absolute of these solutions. Figure 1 illustrates the

behavior of solution (35), which describes a dark optical soliton. Figure 2 depicts the plot of solution (44), which characterizes a bright soliton wave. Figure 3 exhibits the evolution of solution (52), where the graph shows a periodic wave structure. Furthermore, we observe that the plot of solution (56) in Figure 4 represents a bright soliton pulse. One can clearly see that the graph in Figure 5 presents a dark soliton profile, which demonstrates the dynamic behavior of solution (62).

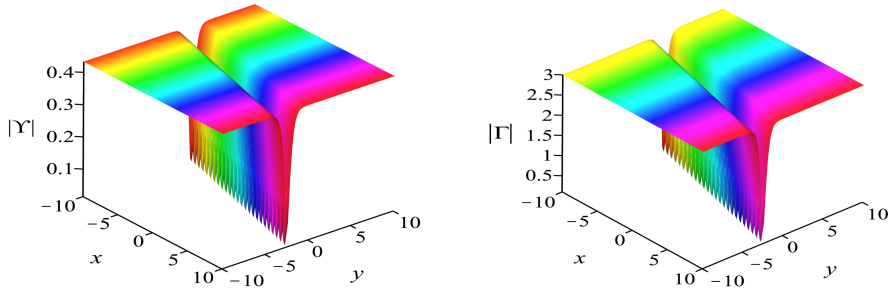

Figure 1. The evolution of solution (35) with $\alpha = 0.5, \beta = \gamma = \omega = B = 2, \nu = \lambda = \eta = \delta = r = 1$, $\sigma = -2, A = -4, z = -0.5$, and $t = 0.1$.

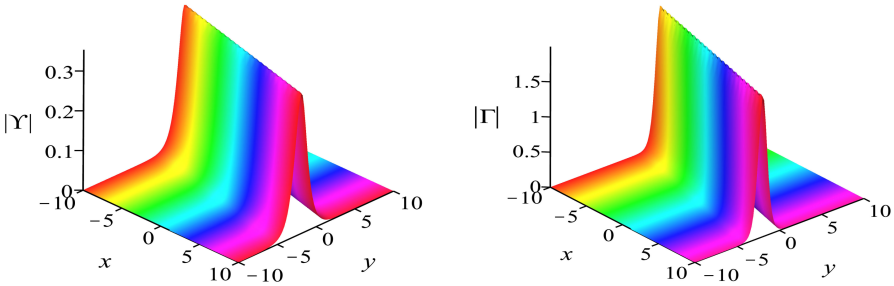

Figure 2. The evolution of solution (44) with $\alpha = 0.5, \beta = \gamma = 2, \nu = \lambda = \eta = 1, \omega = \sigma = -2$, $z = -0.5$, and $t = 0.1$.

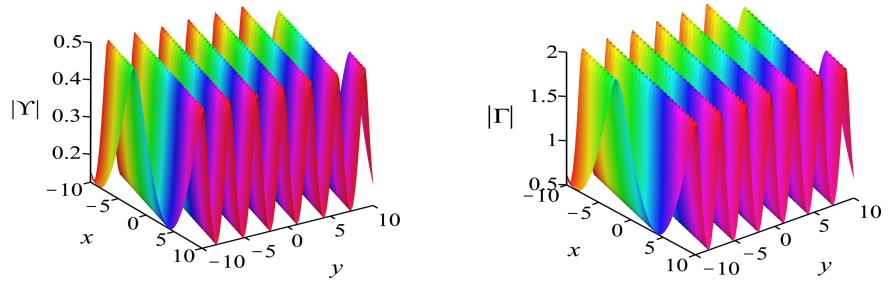

Figure 3. The evolution of solution (52) with $\alpha = 0.5, \beta = \gamma = B = 2, \nu = \lambda = \eta = \delta = 1, \omega = \sigma = -2$, $C = i, z = -0.5$, and $t = 0.1$.

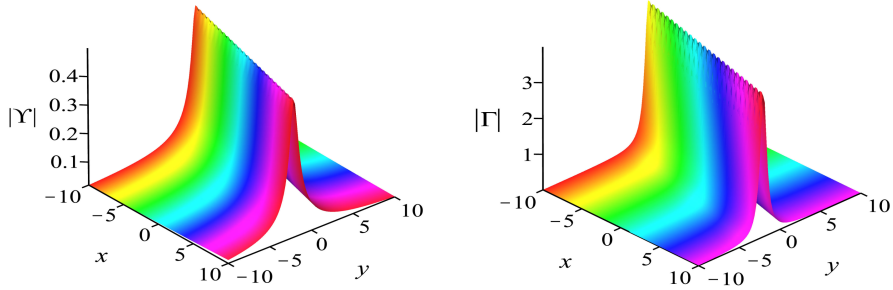

Figure 4. The evolution of solution (56) with $\alpha = 0.5, \beta = \gamma = 2, \nu = \lambda = \eta = p = 1, \omega = \sigma = -2$, $s_2 = i, z = -0.5$, and $t = 0.1$.

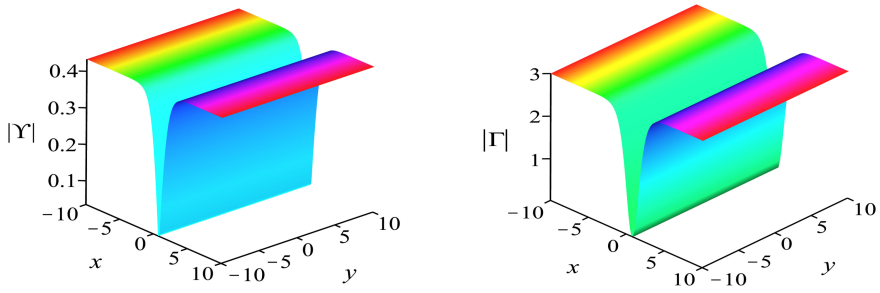

Figure 5. The evolution of solution (62) with $\alpha = 0.5, \beta = \gamma = \omega = 2, \nu = \lambda = \eta = 1, \sigma = -2$, $h = -4$, $z = -0.5$, and $t = 0.1$.

From the presented graphical representations of some obtained solutions, it can be noticed that the optical solitons (bullets) possess various forms of profiles. The rest of the derived solutions may depict miscellaneous soliton structures. In addition, the evolution of optical bullets can be affected by the variations in the physical parameters. In comparison with previous studies [58,59] that scrutinized the 3D-NLSS (2), the optical bullets solutions revealed in this work have different characteristics and behaviors. Hence, these outcomes are expected to contribute to understanding the nature of optical bullets in multidimensional optical media.

7. Conclusions

This work mainly dealt with various optical bullet solutions of a system of (3+1)-dimensional nonlinear Schrödinger equations. After deriving the traveling wave reduction of the system, the resulting equation was handled by means of two powerful techniques called the projective Riccati equations approach and Bernoulli sub-equation function method. Abundant exact solutions having the forms of hyperbolic functions, trigonometric functions, and rational functions were extracted. Consequently, these solutions were found to describe several shapes of optical pulses known as bright, dark, and singular solitons. Additionally, the periodic-type waves were also constructed through some of the retrieved solutions. The dynamic behaviors of some obtained solutions were illustrated to examine the wave structures that emerge in the model. The modulation instability (MI) of the 3D-NLSS was addressed by virtue of the linear stability analysis. It was found that the MI did not exist in the discussed medium. The new recovered results of the 3D-NLSS can be a useful addition to the previous literature and may enhance applications related to the field of fiber optics.

Author Contributions: Conceptualization, K.S.A.-G. and A.B.; methodology, K.S.A.-G. and E.V.K.; software, K.S.A.-G.; validation, K.S.A.-G., E.V.K., S.K., and A.B.; formal analysis, K.S.A.-G. and A.B; writing—original draft preparation, K.S.A.-G.; writing—review and editing, K.S.A.-G., E.V.K., S.K., and A.B.; supervision, A.B. All authors have read and agreed to the published version of the manuscript.

Funding: This research received no external funding.

Institutional Review Board Statement: Not applicable.

Informed Consent Statement: Not applicable.

Data Availability Statement: Not applicable.

Conflicts of Interest: The authors declare no conflict of interest.

References

1. Merzhanov, A.; Khaikin, B. Theory of combustion waves in homogeneous media. *Prog. Energy Combust. Sci.* **1988**, *14*, 1–98. [CrossRef]
2. Swinney, H.L.; Krinsky, V.I. *Waves and Patterns in Chemical and Biological Media*; MIT Press: Cambridge, MA, USA, 1991.
3. Prade, B.; Vinet, J.Y. Guided optical waves in fibers with negative dielectric constant. *J. Light. Technol.* **1994**, *12*, 6–18. [CrossRef]

4. Rose, J.L. Ultrasonic waves in solid media. *J. Acoust. Soc. Am.* **2000**, *107*, 1807. [CrossRef]
5. Brekhovskikh, L. *Waves in Layered Media*; Elsevier: Amsterdam, The Netherlands, 2012; Volume 16.
6. Winterbone, D.E.; Pearson, R.J.; Qatu, M.; Siavoshani, S. Theory of engine manifold design: Wave action methods for ic engineers. *Appl. Mech. Rev.* **2001**, *54*, B109–B110. [CrossRef]
7. Gurnett, D.A.; Bhattacharjee, A. *Introduction to Plasma Physics: With Space and Laboratory Applications*; Cambridge University Press: Cambridge, UK, 2005.
8. Agrawal, G.P. Nonlinear fiber optics. In *Nonlinear Science at the Dawn of the 21st Century*; Springer: Berlin/Heidelberg, Germany, 2000; pp. 195–211.
9. Yariv, A. *Quantum Electronics*; John Wiley & Sons: Abingdon, UK, 1989.
10. Morgan, D. *Surface Acoustic Wave Filters: With Applications to Electronic Communications and Signal Processing*; Academic Press: Cambridge, MA, USA, 2010.
11. Redor, I.; Barthélemy, E.; Michallet, H.; Onorato, M.; Mordant, N. Experimental evidence of a hydrodynamic soliton gas. *Phys. Rev. Lett.* **2019**, *122*, 214502. [CrossRef]
12. Rozenman, G.G.; Fu, S.; Arie, A.; Shemer, L. Quantum mechanical and optical analogies in surface gravity water waves. *Fluids* **2019**, *4*, 96. [CrossRef]
13. Lannig, S.; Schmied, C.M.; Prüfer, M.; Kunkel, P.; Strohmaier, R.; Strobel, H.; Gasenzer, T.; Kevrekidis, P.G.; Oberthaler, M.K. Collisions of three-component vector solitons in Bose-Einstein condensates. *Phys. Rev. Lett.* **2020**, *125*, 170401. [CrossRef]
14. Liu, J.; Lucas, E.; Raja, A.S.; He, J.; Riemensberger, J.; Wang, R.N.; Karpov, M.; Guo, H.; Bouchand, R.; Kippenberg, T.J. Photonic microwave generation in the X-and K-band using integrated soliton microcombs. *Nat. Photonics* **2020**, *14*, 486–491. [CrossRef]
15. Wang, W.; Wang, L.; Zhang, W. Advances in soliton microcomb generation. *Adv. Photonics* **2020**, *2*, 034001. [CrossRef]
16. Rozenman, G.G.; Shemer, L.; Arie, A. Observation of accelerating solitary wavepackets. *Phys. Rev. E* **2020**, *101*, 050201. [CrossRef]
17. Rozenman, G.G.; Schleich, W.P.; Shemer, L.; Arie, A. Periodic Wave Trains in Nonlinear Media: Talbot Revivals, Akhmediev Breathers, and Asymmetry Breaking. *Phys. Rev. Lett.* **2022**, *128*, 214101. [CrossRef] [PubMed]
18. Pernet, N.; St-Jean, P.; Solnyshkov, D.D.; Malpuech, G.; Carlon Zambon, N.; Fontaine, Q.; Real, B.; Jamadi, O.; Lemaître, A.; Morassi, M.; et al. Gap solitons in a one-dimensional driven-dissipative topological lattice. *Nat. Phys.* **2022**, *18*, 678–684. [CrossRef]
19. Qi, Y.; Yang, S.; Wang, J.; Li, L.; Bai, Z.; Wang, Y.; Lv, Z. Recent advance of emerging low-dimensional materials for vector soliton generation in fiber lasers. *Mater. Today Phys.* **2022**, *23*, 100622. [CrossRef]
20. Biswas, A.; Ekici, M.; Sonmezoglu, A.; Belic, M.R. Optical solitons in fiber Bragg gratings with dispersive reflectivity for quadratic–cubic nonlinearity by extended trial function method. *Optik* **2019**, *185*, 50–56. [CrossRef]
21. Al-Ghafri, K.; Krishnan, E.; Biswas, A. W-shaped and other solitons in optical nanofibers. *Results Phys.* **2021**, *23*, 103973. [CrossRef]
22. Al-Kalbani, K.K.; Al-Ghafri, K.; Krishnan, E.; Biswas, A. Solitons and modulation instability of the perturbed Gerdjikov–Ivanov equation with spatio-temporal dispersion. *Chaos Solitons Fractals* **2021**, *153*, 111523. [CrossRef]
23. Zayed, E.M.; Alngar, M.E.; Biswas, A.; Kara, A.H.; Ekici, M.; Alzahrani, A.K.; Belic, M.R. Cubic-quartic optical solitons and conservation laws with Kudryashov's sextic power-law of refractive index. *Optik* **2021**, *227*, 166059. [CrossRef]
24. Hosseini, K.; Osman, M.; Mirzazadeh, M.; Rabiei, F. Investigation of different wave structures to the generalized third-order nonlinear Scrödinger equation. *Optik* **2020**, *206*, 164259. [CrossRef]
25. Al-Kalbani, K.K.; Al-Ghafri, K.; Krishnan, E.; Biswas, A. Pure-cubic optical solitons by Jacobi's elliptic function approach. *Optik* **2021**, *243*, 167404. [CrossRef]
26. Ekici, M.; Sonmezoglu, A.; Biswas, A.; Belic, M.R. Optical solitons in (2+1)–Dimensions with Kundu–Mukherjee–Naskar equation by extended trial function scheme. *Chin. J. Phys.* **2019**, *57*, 72–77. [CrossRef]
27. Krishnan, E.; Biswas, A.; Zhou, Q.; Alfiras, M. Optical soliton perturbation with Fokas–Lenells equation by mapping methods. *Optik* **2019**, *178*, 104–110. [CrossRef]
28. Kudryashov, N.A. Periodic and solitary waves in optical fiber Bragg gratings with dispersive reflectivity. *Chin. J. Phys.* **2020**, *66*, 401–405. [CrossRef]
29. Zayed, E.M.; Alngar, M.E. Application of newly proposed sub-ODE method to locate chirped optical solitons to Triki–Biswas equation. *Optik* **2020**, *207*, 164360. [CrossRef]
30. Yıldırım, Y.; Topkara, E.; Biswas, A.; Triki, H.; Ekici, M.; Guggilla, P.; Khan, S.; Belic, M.R. Cubic–quartic optical soliton perturbation with Lakshmanan–Porsezian–Daniel model by sine-Gordon equation approach. *J. Opt.* **2021**, *50*, 322–329. [CrossRef]
31. Silberberg, Y. Collapse of optical pulses. *Opt. Lett.* **1990**, *15*, 1282–1284. [CrossRef]
32. Biswas, A. Theory of Optical Bullets. *PIER* **2002**, *36*, 21–59. [CrossRef]
33. Soto-Crespo, J.M.; Grelu, P.; Akhmediev, N. Optical bullets and "rockets" in nonlinear dissipative systems and their transformations and interactions. *Opt. Express* **2006**, *14*, 4013–4025. [CrossRef]
34. Smetanina, E.; Kompanets, V.; Dormidonov, A.; Chekalin, S.; Kandidov, V. Light bullets from near-IR filament in fused silica. *Laser Phys. Lett.* **2013**, *10*, 105401. [CrossRef]
35. Dormidonov, A.; Kompanets, V.; Chekalin, S.; Kandidov, V. Giantically blue-shifted visible light in femtosecond mid-IR filament in fluorides. *Opt. Express* **2015**, *23*, 29202–29210. [CrossRef]

36. Chekalin, S.V.; Kompanets, V.O.; Dormidono, A.; Kandidov, V.P. Light bullet dynamics in uniform dielectrics:(50th anniversary of the Institute of Spectroscopy, Russian Academy of Sciences). *Phys.-Uspekhi* **2019**, *62*, 282. [CrossRef]
37. Shumakova, V.; Ališauskas, S.; Baltuška, A.; Malevich, P.; Voronin, A.; Mitrofanov, A.; Sidorov-Biryukov, D.; Zheltikov, A.; Kartashov, D.; Pugžlys, A. Multi-mJ mid-IR light bullets in air. *EPJ Web Conf.* **2019**, *205*, 01004. [CrossRef]
38. Zaloznaya, E.D.; Kompanets, V.O.; Chekalin, S.V.; Dormidonov, A.E.; Kandidov, V.P. Interference effects in the formation of the light bullet spectrum under axicon focusing. *Quantum Electron.* **2020**, *50*, 366. [CrossRef]
39. Blagoeva, A.; Dinev, S.; Dreischuh, A.; Naidenov, A. Light bullets formation in a bulk media. *IEEE J. Quantum Electron.* **1991**, *27*, 2060–2065. [CrossRef]
40. Malomed, B.A.; Drummond, P.; He, H.; Berntson, A.; Anderson, D.; Lisak, M. Spatiotemporal solitons in multidimensional optical media with a quadratic nonlinearity. *Phys. Rev. E* **1997**, *56*, 4725. [CrossRef]
41. Fibich, G.; Ilan, B. Optical light bullets in a pure Kerr medium. *Opt. Lett.* **2004**, *29*, 887–889. [CrossRef]
42. Belić, M.; Petrović, N.; Zhong, W.P.; Xie, R.H.; Chen, G. Analytical light bullet solutions to the generalized (3+1)-dimensional nonlinear Schrödinger equation. *Phys. Rev. Lett.* **2008**, *101*, 123904. [CrossRef]
43. Petrović, N.Z.; Belić, M.; Zhong, W.P.; Xie, R.H.; Chen, G. Exact spatiotemporal wave and soliton solutions to the generalized (3+1)-dimensional Schrödinger equation for both normal and anomalous dispersion. *Opt. Lett.* **2009**, *34*, 1609–1611. [CrossRef]
44. Minardi, S.; Eilenberger, F.; Kartashov, Y.V.; Szameit, A.; Röpke, U.; Kobelke, J.; Schuster, K.; Bartelt, H.; Nolte, S.; Torner, L.; et al. Three-dimensional light bullets in arrays of waveguides. *Phys. Rev. Lett.* **2010**, *105*, 263901. [CrossRef]
45. Belyaeva, T.; Hasegawa, A.; Kovachev, L.; Serkin, V. 3D soliton-like bullets in nonlinear optics and Bose-Einstein condensates. In *Proceedings of the 16th International School on Quantum Electronics: Laser Physics and Applications*; SPIE: Bellingham, WA, USA, 2011; Volume 7747, pp. 343–352.
46. He, J.; Song, Y.; Tiofack, C.; Taki, M. Rogue wave light bullets of the three-dimensional inhomogeneous nonlinear Schrödinger equation. *Photonics Res.* **2021**, *9*, 643–648. [CrossRef]
47. Khalyapin, V.; Bugay, A. Analytical study of light bullets stabilization in the ionized medium. *Chaos Solitons Fractals* **2022**, *156*, 111799. [CrossRef]
48. Radha, R.; Lakshmanan, M. Singularity structure analysis and bilinear form of a (2+1) dimensional non-linear Schrodinger (NLS) equation. *Inverse Probl.* **1994**, *10*, L29. [CrossRef]
49. Liu, C.; Wang, Z.; Dai, Z.; Chen, L. Rogue waves in the (2+1)-dimensional nonlinear Schrodinger equations. *Int. J. Numer. Methods Heat Fluid Flow* **2015**, *25*, 656–664. [CrossRef]
50. Zhang, H.Q.; Liu, X.L.; Wen, L.L. Soliton, breather, and rogue wave for a (2+1)-dimensional nonlinear Schrödinger equation. *Z. Für Naturforschung A* **2016**, *71*, 95–101. [CrossRef]
51. Rao, J.; Wang, L.; Liu, W.; He, J. Rogue-wave solutions of the Zakharov equation. *Theor. Math. Phys.* **2017**, *193*, 1783–1800. [CrossRef]
52. Liu, Y.K.; Li, B. Rogue waves in the (2+1)-dimensional nonlinear Schrödinger equation with a parity-time-symmetric potential. *Chin. Phys. Lett.* **2017**, *34*, 010202. [CrossRef]
53. Wang, J.; Chen, L.; Liu, C. Bifurcations and travelling wave solutions of a (2+1)-dimensional nonlinear Schrödinger equation. *Appl. Math. Comput.* **2014**, *249*, 76–80. [CrossRef]
54. Gao, W.; Hu, Y. Traveling wave solutions of a nonlinear Schrödinger type equation by using first integral method. In Proceedings of the 2017 29th Chinese Control And Decision Conference (CCDC), Chongqing, China, 28–30 May 2017; pp. 6349–6354.
55. Seadawy, A.R.; Cheemaa, N.; Biswas, A. Optical dromions and domain walls in (2+1)-dimensional coupled system. *Optik* **2021**, *227*, 165669. [CrossRef]
56. Hosseini, K.; Sadri, K.; Mirzazadeh, M.; Salahshour, S. An integrable (2+1)-dimensional nonlinear Schrödinger system and its optical soliton solutions. *Optik* **2021**, *229*, 166247. [CrossRef]
57. Çankal, P.D.; Yaşar, E. Optical soliton solutions to a (2+1) dimensional Schrödinger equation using a couple of integration architectures. *Appl. Math. Nonlinear Sci.* **2021**, *6*, 381–396. [CrossRef]
58. Borzykh, A.V. The Hirota Method and Soliton Solutions to the Multidimensional Nonlinear Schrodinger Equation. *Sib. Math. J.* **2002**, *43*, 212–214. [CrossRef]
59. Zhang, J.; Shen, S. Exact solutions of some nonlinear evolution systems. *Phys. Lett. A* **2006**, *355*, 465–467. [CrossRef]
60. Wazwaz, A.M. The tanh method for traveling wave solutions of nonlinear equations. *Appl. Math. Comput.* **2004**, *154*, 713–723. [CrossRef]
61. Zayed, E.; Gepreel, K.A. The (G'/G)-expansion method for finding traveling wave solutions of nonlinear partial differential equations in mathematical physics. *J. Math. Phys.* **2009**, *50*, 013502. [CrossRef]